Pharmaceutical Research, Vol. 23, No. 12, December 2006 (© 2006)
DOI: 10.1007/s11095-006-9100-8

Research Paper

Mechanisms Responsible for Poor Oral Bioavailability of Paeoniflorin: Role of Intestinal Disposition and Interactions with Sinomenine

Zhong Qiu Liu,[1,2] Zhi Hong Jiang,[2] Liang Liu,[2,3] and Ming Hu[1,3]

Received April 6, 2006; accepted June 26, 2006; published online October 25, 2006

Purpose. To determine the intestinal disposition mechanisms of paeoniflorin, a bioactive glucoside, and to investigate the mechanisms by which sinomenine increases paeoniflorin bioavailability.
Materials and Methods. A single-pass "four-site" rat intestinal perfusion model and a cultured Caco-2 cell model were employed.
Results. In both model systems, paeoniflorin permeability was poor. In the perfusion model, maximal absorption and metabolism of paeoniflorin occurred in duodenum and jejunum, which were significantly decreased by a glucosidase inhibitor gluconolactone (20 mM). On the other hand, paeoniflorin absorption in terminal ileum increased significantly but its metabolism did not in the presence of sinomenine and cyclosporine A. In the Caco-2 cell model, paeoniflorin was transported 48-fold slower than its aglycone (paeoniflorigenin). Absorptive transport of paeoniflorin was significantly ($p < 0.05$) increased by sinomenine (38%), verapamil (27%), and cyclosporine A (41%), whereas its secretory transport was significantly ($p < 0.01$) decreased by sinomenine (50%), verapamil (35%) and cyclosporine A (37%). In contrast, MRP inhibitors MK-571 and leukotriene C4 did not affect transport of paeoniflorin. Lastly, sinomenine was also shown to significantly increase the absorptive transport of digoxin (a prototypical p-glycoprotein substrate) and to significantly decrease its secretory transport.
Conclusions. Poor permeation, p-gp-mediated efflux, and hydrolysis via a glucosidase contributed to the poor bioavailability of paeoniflorin. Sinomenine (an inhibitor of the p-gp-mediated digoxin efflux) increased paeoniflorin's bioavailability via the inhibition of p-gp-mediated paeoniflorin efflux in the intestine.

KEY WORDS: bioavailability; Caco-2; disposition; efflux; intestinal; paeoniflorin; p-glycoprotein inhibitor; sinomenine.

INTRODUCTION

Paeoniflorin is a bioactive and water soluble monoterpene glucoside (MW: 428.47, Fig. 1), present in the root of a Chinese medicinal herb *Paeonia lactiflora* Pall. The herb is widely used to treat inflammatory conditions, and the enriched *P. lactiflora* containing 70% paeoniflorin is an approved proprietary drug for treatment of rheumatic and arthritic diseases by the State Food and Drugs Administration of China. The therapeutic effects of its active component, paeoniflorin, have been demonstrated by many investigators (1,2). However, use of paeoniflorin in Chinese clinic is limited because it has poor bioavailability, which was attributed to poor permeation by passive diffusion since its log *P* value is −2.88.

Previous studies had reported low bioavailability of orally administered paeoniflorin in rats (approximately 3–4%) (3,4), and our own pharmacokinetic study was consistent with this observation (5). An earlier study indicated that higher plasma concentrations of paeoniflorin were achieved by using a more crude extract of the plant (6). Additional reports showed that higher plasma concentrations of paeoniflorin were achieved when it is included as a part of multiple herb formula: *Shao-yao Gan-chao Tang* (6,7). These results indicated that the bioavailability of paeoniflorin could be improved by other phytochemicals present in the herb or herbal formulations.

With regard to the disposition of paeoniflorin, it was found that this compound was not absorbed intact and only aglycone paeoniflorgenin was absorbable into the systemic circulation in rats (8). Administered paeoniflorin was extensively metabolized into paeoniflorgenin, paeonimetabolins I and II (Fig. 1). The mechanism responsible for the formation of paeoniflorgenin is unknown but formation of all three metabolites was assumed to be catalyzed by intestinal microflora (9,10).

To determine the causes of its low bioavailability, we found earlier using an everted sac model of rat intestine that poor uptake and efflux contributed to this poor bioavailability (11). However, the everted gut sac model is not best suited to

[1] Department of Pharmacological and Pharmaceutical Sciences, College of Pharmacy, University of Houston, Houston, Texas 77030, USA.
[2] School of Chinese Medicine, Hong Kong Baptist University, Kowloon Tong, Hong Kong, People's Republic of China.
[3] To whom correspondence should be addressed. (e-mail: mhu@uh.edu; Liuliang@hkbu.edu.hk)

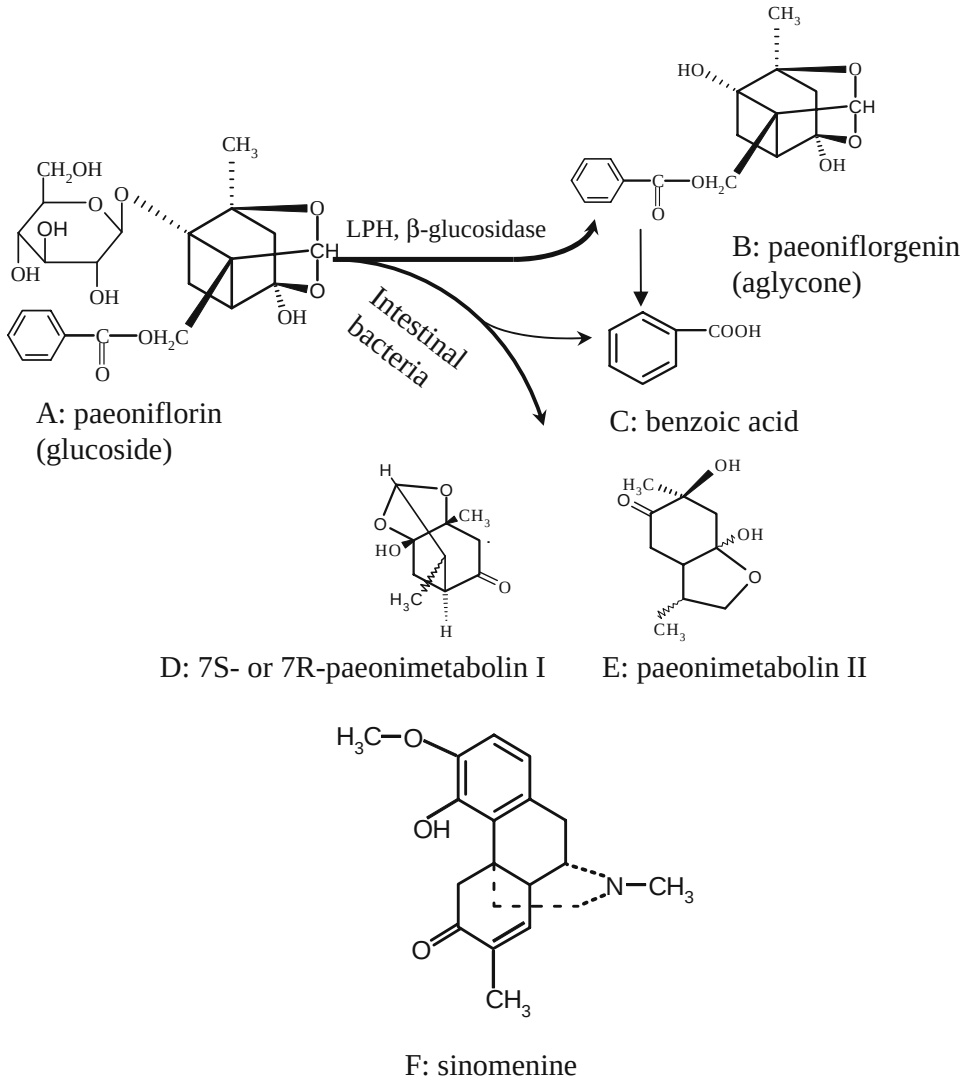

Fig. 1. Structure of compounds used in the present study and proposed metabolic pathways of paeoniflorin in the intestine.

study slowly transported compound such as paeoniflorin as viability was a significant challenge when study has to be run for more than 30 min. Therefore, one goal of present study was to further understand why paeoniflorin has poor bioavailability using an *in situ* perfusion model where tissue integrity and blood circulation are maintained. Additional, a human intestinal Caco-2 model was used to determine if the mechanism elucidated in rat intestine is relevant in the human intestine.

To determine how we could increase the bioavailability of paeoniflorin, we used sinomenine, a bioactive alkaloid derived from *Sinomenium acutum* Rehdder & Wilson, that is also used to treat rheumatic and arthritic diseases in China. Sinomenine has a variety of actions including anti-inflammation (12,13), immunosuppression (14), and arthritis amelioration (15). In a previous study, we demonstrated that co-administration of sinomenine could markedly elevate the plasma concentration of paeoniflorin (5) and that addition of this compound in the incubation media increased the uptake of paeoniflorin in a rat everted gut sac model (9). Therefore, the second goal of this study was to investigate the mechanisms by which sinomenine increases the bioavailability of paeoniflorin, which would help us understand how to improve its pharmacokinetic profile.

MATERIALS AND METHODS

Materials

Cloned Caco-2 cells (TC7) were a kind gift from Dr. Monique Rousset (Institut National de la Sante et de la Recherche Medicale U178, Villejuit, France). Paeoniflorin and sinomenine (≧98% in purity, see Fig. 1 for structure) were purchased from the State Institute for Control of Biological and Pharmaceutical Products (Beijing, China). Pentoxifylline (an internal standard or IS with greater than 98% purity), β-glucosidase, gluconolactone, Hanks' balanced salt solution (HBSS; powder form), verapamil and cyclosporine A were obtained from Sigma-Aldrich Chemical (St. Louis, MO, USA).

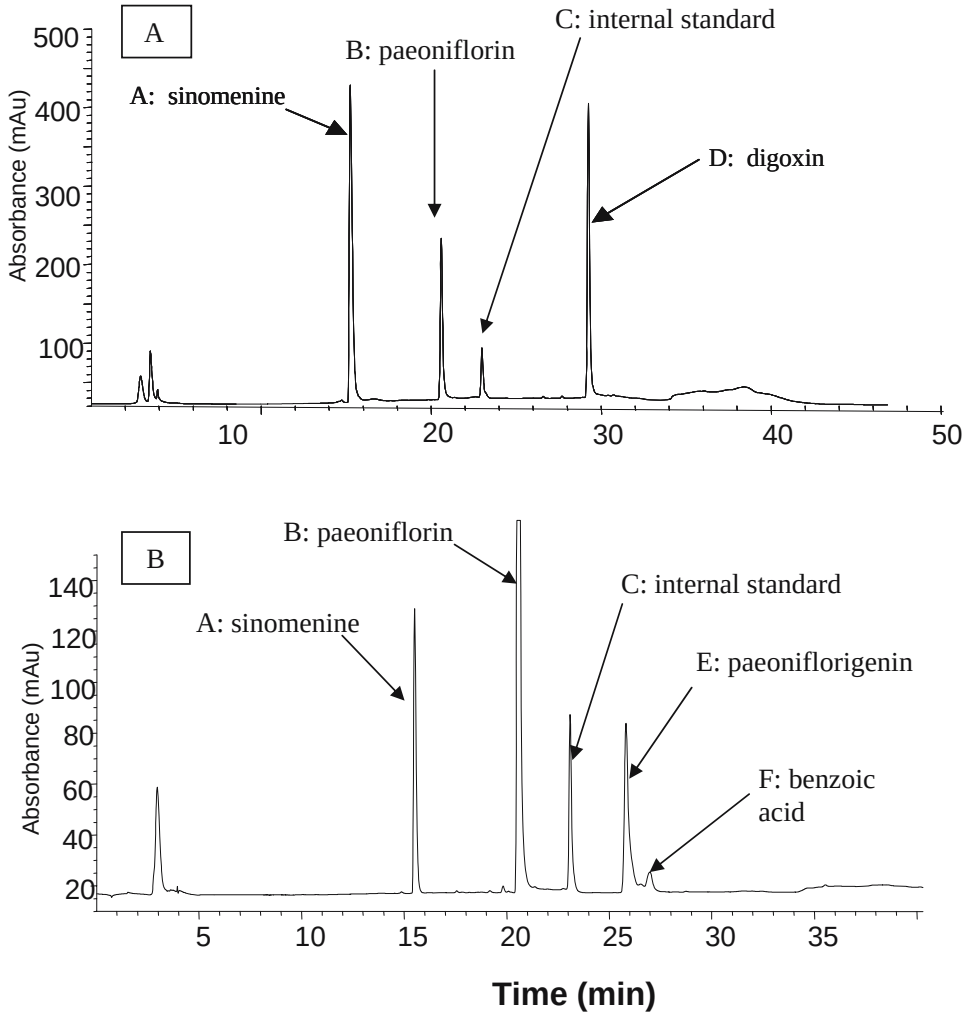

Fig. 2. Representative HPLC profiles of transport samples in the Caco-2 cell culture model (A) and the perfusion samples in the rat intestinal perfusion model (B). Using the HPLC analysis method described in the text, accuracy and precision for the assay were determined and validated using sinomenine, paeoniflorin and digoxin at 0.78, 25, 100 μM (triplicates for each concentration). The results showed the method had a good accuracy and precision (data not shown). Calibration curves were plotted as the peak area *vs* drug concentration. Results for the calibration curves ($n = 8$) showed good linearity (all of r^2 were over 0.999) in the concentration range of 0.78–100 μM for all three compounds.

Cell Culture

The culture conditions for growing Caco-2 cells (passage number: 30-48 generation) have been described previously (16–18). The seeding density, growth media (Dulbecco's modified Eagle's medium supplemented with 10% fetal bovine serum), and quality control criteria were all implemented in the present study as they were described previously (16–18). TC7 cells were fed every other day, and cell monolayers (4.2 cm^2 total areas) were ready for experiments from 19 to 22 days after seeding.

Transport Experiments in the Caco-2 Cell Culture Model

Experiments in triplicate were performed in HBSS (16,17). Transport experiments were performed using pH 6.5 (which is jejunal pH) at the apical side and pH 7.4 (which is the serosal pH) at the basolateral side unless otherwise specified. The protocols for performing cell culture experiments were similar to those described previously (16–18). Briefly, the cell monolayers were washed three times with 37°C pH 7.4 HBSS. The transepithelial electrical resistance values of Caco-2 cell monolayers were measured, and those monolayers with transepithelial electrical resistance values less than 420 ohm cm^2 were not used. The monolayers were loaded with a solution containing the compound of interest, and the amount of transepithelial transported was followed as a function of time by HPLC. Four samples (0.5 ml/per sample) were taken at different times, which were immediately added acetonitrile (0.125 ml/per sample) containing IS (16 μM) to stabilize the test compounds, and the amounts transported were determined by HPLC.

Cellular Accumulation Studies in the Cell Monolayers

When the transport experiments were completed, the mature monolayers (three inserts/group) were gently and softly washed three time with iced HBSS buffer (pH 7.4), they

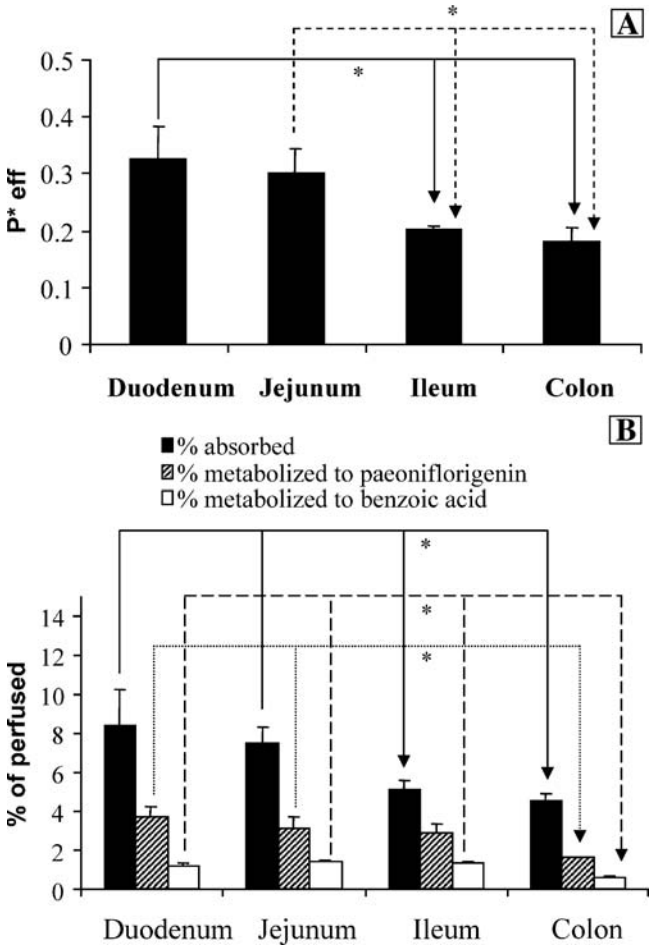

Fig. 3. Effective dimensionless permeabilities of paeoniflorin (A), percentages of metabolite (paeoniflorigenin and benzoic acid) found in the perfusate (B) in four regions of the rat intestine (duodenum, jejunum, terminal ileum and colon) that were perfused at a flow rate of 0.15 ml/min. In all perfusion studies, effective permeability (P^*_{eff}), percentages of paeoniflorin absorbed and metabolites formed or excreted (the latter two normalized to a 10-cm intestinal length) were calculated using equations described in the "Materials and Methods section." Statistically significant differences ($p < 0.05$) between regions were shown by the *asterisks* (*). In (B), we performed one-way ANOVA with post hoc test and significant differences in the pairs were marked by the *arrow* and the *asterisks* (*). Each column represents the average of four determinations and the *error bar* represents the standard error of the mean.

were cut out together with the porous polycarbonate membranes, immersed into 0.5 ml of 50-mM potassium phosphate buffer (pH 7.4) and sonicated in an ice bath (4°C) for 15 min as described previously (19). Amounts of drugs in the lysate were then determined by HPLC.

Animals

Male Sprague–Dawley rats aging 70 to 110 days old and weighing between 250–350 g (Harlan Laboratory, Indianapolis, Indiana) were used. The rats were fed with Teklad F6 rodent diet (W) from Harlan Bioproducts for Science (Indianapolis, IN). The rats were fasted overnight before the date of the experiment.

Animal Surgery

The procedures were approved by University of Houston's Institutional Animal Care and Uses Committee. The intestinal surgical procedures were modified from our previous publication (21,22), in that we perfused four segments of the intestine simultaneously (a "four-site model"). In the present study, the cannulation to the duodenum, jejunum, ileum, and colon, respectively, was connected to a short cannulae, which was 1.5 to 2 cm long and can be easily disconnected or reconnected to the main perfusion tube. The main tube was attached to a syringe driven by an infusion pump (Model PHD 2000;

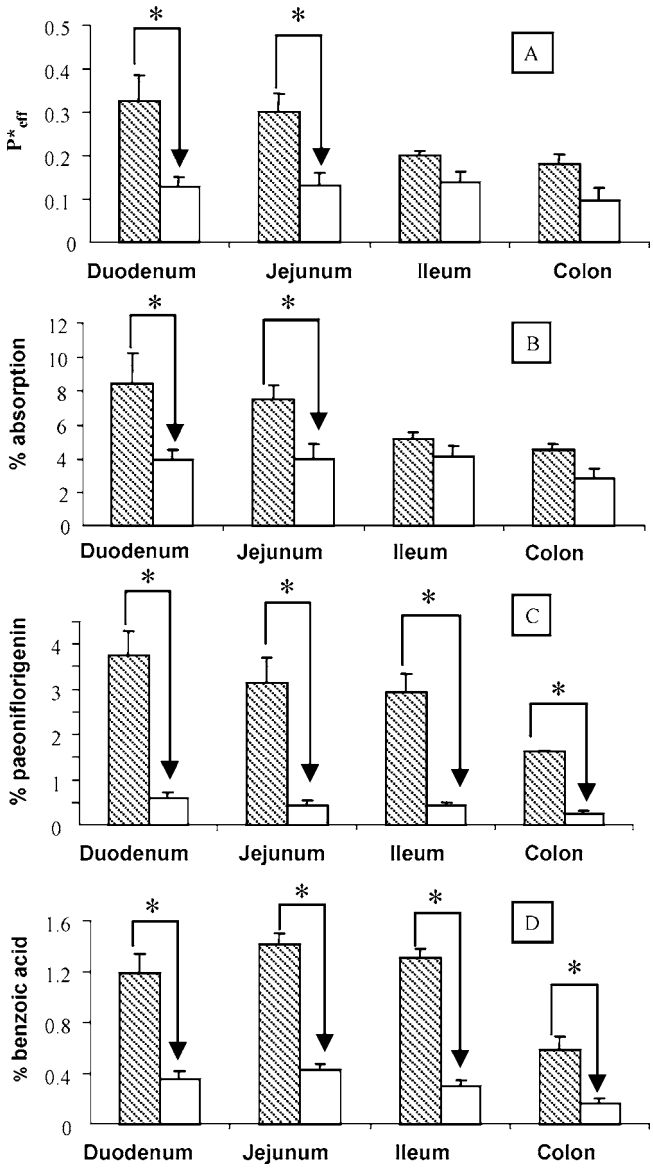

Fig. 4. Effective dimensionless permeabilities of paeoniflorin (A), percentages of paeoniflorin absorbed (B), percentages of paeoniflorigenin found in perfusate (C) or percentage of benzoic acid excreted by enterocytes (D) in four regions of the rat intestine in the absence (*slashed bars*) or presence (*open bars*) of 20-mM gluconolactone. Statistically significant differences ($p < 0.05$) between gluconolactone treatment were marked by the *asterisks* (*) using unpaired Student's *t*-test. Each column represents the average of four determinations and the *error bar* represents the standard error of the mean.

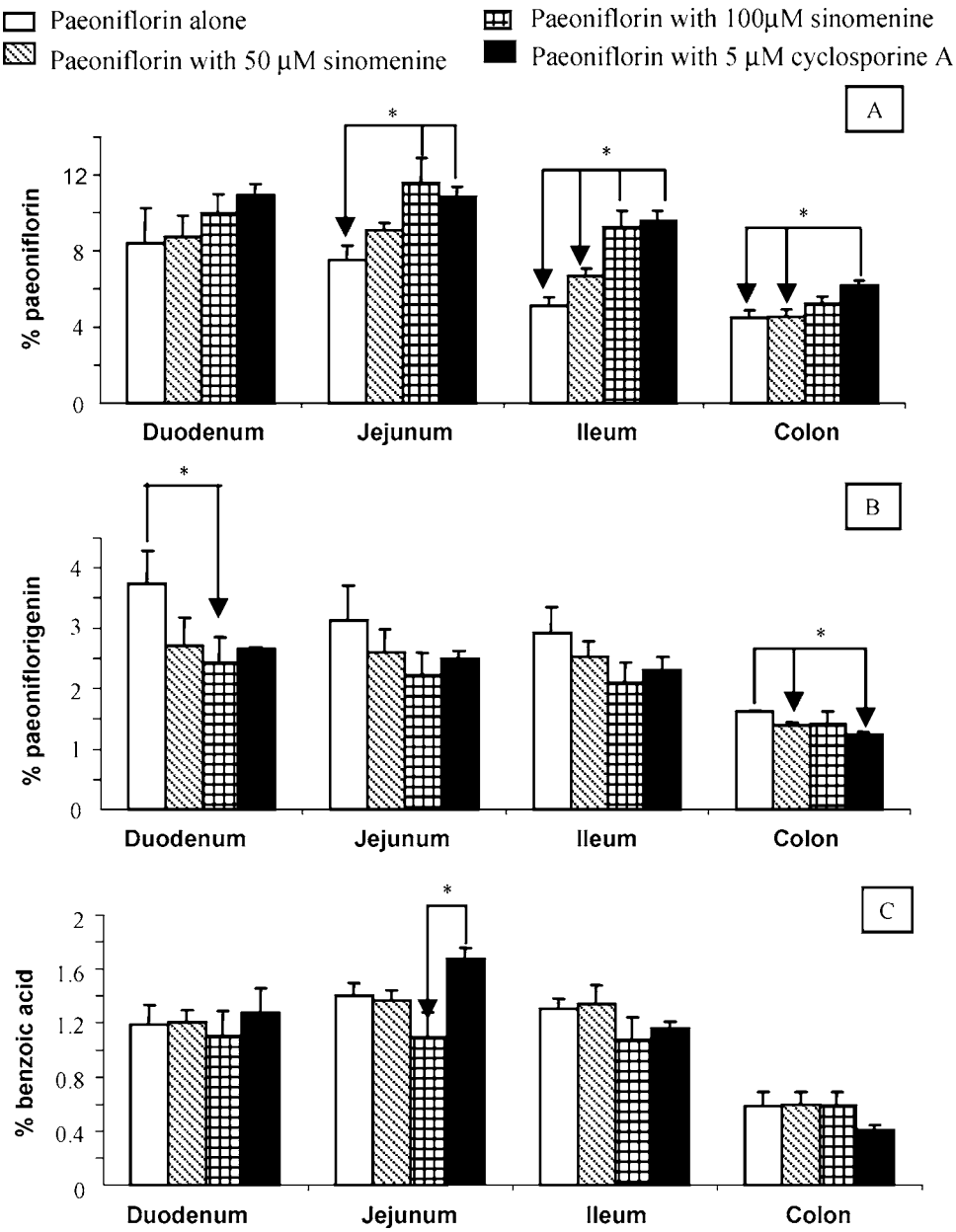

Fig. 5. Effects of sinomenine or p-gp inhibitors on the absorption and metabolism of paeoniflorin in the rat intestine. Formation of metabolites and absorption of paeoniflorin were determined using perfusate containing paeoniflorin alone (50 μM alone, *open columns*), or with 50-μM sinomenine (*slashed columns*), or with 100-μM sinomenine (*checkered* columns), or 5-μM cyclosporine A (*solid columns*). The *asterisk* (*) indicates a statistically significant difference ($P < 0.05$) when compared to the control according to a one-way ANOVA with post hoc test. *Each column* represents the average of four determinations, and the *error bar* represents the standard error of the mean.

Harvard Apparatus, Cambridge, MA). To keep the temperature of the perfusate constant, the inlet cannula was insulated and kept warm by a 37°C circulating water bath.

Transport and Metabolism Experiments in the Perfused Rat Intestinal Model

A single-pass perfusion method described previously was used (18,20). A flow rate of 0.15 ml/min was used, and four perfusate samples were collected every 30 min as described (18,20). The outlet concentrations of test compounds in the perfusate were determined by HPLC.

Preparation of Paeoniflorigenin (Aglycone) from Paeoniflorin (Glucoside)

Paeoniflorin (100 mg) was dissolved in 0.2 ml of dimethyl sulfoxide, to which 2.5 ml of β-glucosidase (100 U/ml) was added. The reaction was allowed to continue for 5 hr in a shaking water bath (37°C, 100 rpm). Afterwards, the mixture

was extracted twice with ethyl acetate. The combined ethyl acetate layer was evaporated to dryness. The residue was redissolved in 1 ml methanol and chromatographed over ODS stationary phase (Merck, USA) using increasing concentration of methanol in water as the eluent. This procedure yielded ten fractions, which were then analyzed for paeoniflorigenin by HPLC. The fraction eluted with 30% methanol contained pure paeoniflorigenin. This fraction was then further processed to yield pure aglycone (5 mg) (8).

HPLC Analysis of Digoxin, Paeoniflorin and Sinomenine

Digoxin, paeoniflorin and sinomenine were analyzed via HPLC after samples were centrifuged at 13,000 rpm for 10 min. The HPLC conditions were as follows: system, Agilent 1050 controlled by Chemstation with a 759A absorbance detector (Applied Biosystems, AB); column, Altima C_{18} column (dimensions of 250 × 4.5 mm, particle size of 5 μm). For the analysis of Caco-2 samples, the HPLC conditions are: mobile phase A, 100% acetonitrile; mobile phase B, 0.05% (v/v) acetic acid in water; gradient, 0–5 min, 5% A, 5–26 min, 5–35% A, 30–35 min, 35% A, 35–36 min 35–5% A. For the perfusate samples, the HPLC conditions are: mobile phase A, 100% acetonitrile; mobile phase B, water (0.04% phosphoric acid and 0.09% triethylamine, pH 6.0); gradient, 0–5 min, 5%A, 5–26 min, 5–40% A, 30–35 min, 40% A, 35–36 min 40–5% A; the detection wavelength, 231 nm for all compounds; and injection volume, 200 μl. All tested compounds have linear response ranges from 0.78 to 100 μM. Retention times for sinomenine, paeoniflorin, internal standard and digoxin in the Caco-2 cell transport samples were 14.6, 20.5, 23.5 and 29.5 min, respectively (Fig. 2A). Retention times for sinomenine, paeoniflorin, internal standard, paeoniflorigenin and benzoic acid in the perfusate samples were 15.1, 21.5, 23.5 and 26.5 and 27.9 min, respectively (Fig. 2B).

Data Analysis in the Caco-2 Cell Culture Model

The apparent unidirectional permeability was obtained according to the following equation (Eq. 1):

$$\frac{B_t}{SC} = P_{app} \tag{1}$$

Where B_t is the apparent appearance rate of drug molecules in the receiver side, S is the surface area of the monolayer (4.2 cm^2), and C is the starting concentration in the donor side. The flux term B_t was calculated using linear regression (a Microsoft Excel function).

Rate of transport (B_t) was obtained using rate of change in concentration of transported paeoniflorin as a function of time and volume of the sampling chamber (V) (Eq. 2).

$$\frac{dC}{dt}V = B_t \tag{2}$$

Data Analysis in the Rat Intestinal Perfusion Model

In the intestinal model, effective permeability (P^*_{eff}) was calculated using an equation described previously (18,21,22). Amount of paeoniflorin absorbed (M_{ab}) was expressed as follows:

$$M_{ab} = Q\tau(CA_{in} - CA_{out}) \tag{3}$$

Where Q is the flow rate (in milliliters per minute), τ is the sampling interval (30 min), and CA_{in} and CA_{out} are the inlet and outlet concentrations of paeoniflorin corrected for water flux, respectively.

Amounts of metabolites found in the intestinal lumen (M_{gut}) were expressed as follows: where CM_{out} is the outlet concentrations (in nanomoles per milliliter) of metabolites corrected for water flux, and Q and τ are the same as defined for Eq. (3).

$$M_{gut} = Q\tau(CM_{out}) \tag{4}$$

The percent absorbed and percent metabolized values were calculated as follows:

$$\%\ \text{absorbed in the intestine} = M_{ab}/M_{total} \tag{5}$$

$$\%\ \text{metabolites found in intestine} = M_{gut}/M_{total} \tag{6}$$

where M_{total} is the total amount of compound perfused over a 30-min time period.

Statistical Analysis

One-way ANOVA with post hoc test for multiple comparisons (SPSS 11.5) and unpaired Student's t test (Microsoft Excel) for double comparisons were used to analyze the data. The prior level of significance was set at 5%, or $p < 0.05$.

RESULTS

The presentation of the results will be divided into two sections: rat perfusion studies and Caco-2 cell studies.

Rat Perfusion Studies

Our previous study *in vivo* using the Sprague–Dawley rats showed that paeoniflorin had a poor bioavailability (5). In order to be consistent with the *in vivo* experiments, we chose the same strain of rats for the present study. Using the intestinal perfusion model, we investigated the absorption and metabolism of paeoniflorin in the intestine.

Regional Absorption and Metabolism of Paeoniflorin

There were significant differences (one-way ANOVA with post hoc test, $p < 0.05$) in the amounts of paeoniflorin absorbed from different regions of the intestine when 50-μM paeoniflorin was perfused (Fig. 3). Furthermore, another parameter, the apparent dimensionless effective permeabilities or P^*_{eff} of paeoniflorin, in upper small intestine (i.e., duodenum and jejunum) were higher than those in terminal ileum and colon (Fig. 3). There were also significant differences in metabolites found from different regions of the

Table I. Effects of Concentration on the Transepithelial Transport of Paeoniflorin

	Permeability (10^{-6} cm/s)		Rate of transport (pmol min^{-1} cm^{-2})		
Paeoniflorin (μM)	A-B (mean ± SD)	B-A (mean ± SD)	AP-to-BL (mean ± SD)	BL-to-AP (mean ± SD)	Ratio(B-A/A-B)
100	0.483 ± 0.018	1.396 ± 0.083***	2.94 ± 0.11	8.13 ± 0.48 ***	2.76
200	0.364 ± 0.024	1.084 ± 0.010**	3.93 ± 0.25	11.66 ± 1.09**	2.97
400	0.258 ± 0.030	0.763 ± 0.030***	5.62 ± 0.64	16.88 ± 0.67 ***	3.01
800	0.223 ± 0.039	0.772 ± 0.106**	12.32 ± 1.76	42.62 ± 7.20 **	3.46

Experiments were performed at 37°C for 240 min. Donor and receiver volumes were 2.5 ml. The donor buffer was pH 6.5 HBSS and the receiver buffer was pH 7.4 HBSS. The rate of transepithelial transport values for both AP-to-BL and BL-to-AP transport were calculated as described in the Materials and Methods section. Data are expressed as mean ± SD, and $n = 3$. The statistically significant difference is between the BL-to-AP rate of transport and the AP-to-BL rate of transport at various tested concentrations.
***$p < 0.001$.
**$p < 0.01$.

intestine. For paeoniflorigenin, the % formed was the highest in rat duodenum, followed by jejunum and terminal ileum, all of which are significantly higher than colon ($p < 0.05$) (Fig 3). Percentage of another metabolite, benzoic acid, excreted by the small intestine were also higher than that by the colon ($p < 0.05$) (Fig. 3).

Aside from being absorbed and metabolized, paeoniflorin has minimal effects on water flux (i.e., less than 0.5%/cm of perfused intestinal segment), regardless of whether inhibitors were used or not. The lack of effect on water flux is similar to results previously observed in the rat perfusion model, suggesting that paeoniflorin or its metabolites were not acutely toxic (18,19).

Regional Absorption and Metabolism of Paeoniflorin in the Presence of LPH Inhibitor Gluconolactone

Lactase phlorizin hydrolase or LPH has been shown to be responsible for the hydrolysis of flavonoid glucosides (19,25). Since paeoniflorin is a glucoside of paeoniflorigenin, and hydrolysis of paeoniflorin to its aglycone occurred in the outlet perfusate, we determined how a LPH inhibitor gluconolactone would affect its absorption. As expected, the absorption of paeoniflorin (50 μM) in the upper small intestine, where LPH is abundantly expressed (23), decreased significantly in the presence of gluconolactone (20 mM) (Fig. 4). Furthermore, the regional difference in absorption of paeoniflorin disappeared in the presence of gluconolactone. Interestingly, the extent of decrease in metabolite found in the perfusate (≈85%) was more pronounced than the extent of decrease in absorption in the upper small intestine (up to 50%). Furthermore, the % decreases in excreted metabolites were significant in all regions of the intestine including the colon.

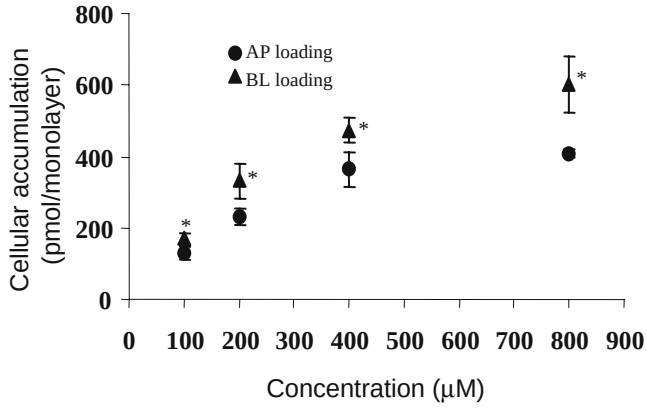

Fig. 6. Effect of concentration on the cellular accumulation of paeoniflorin. Experiments were performed over a 4-h period at 37°C with apical loading: *filled circles* (●) or basolateral loading: *filled triangles* (▲). The amounts that accumulated were measured after the cell monolayers were washed three times with ice-cold saline solution. The *asterisk* (*) indicates a statistically significant difference between apical and basolateral loadings at the tested concentration. Each data point is the average of three determinations, and the *error bars* represent the standard deviation of the mean.

Effects of Sinomenine and P-gp Inhibitor on Absorption and Metabolism of Paeoniflorin

Absorption and metabolism of paeoniflorin was determined in the absence or presence of a p-gp efflux transporter inhibitor cyclosporine A (5 μM) or sinomenine (100 μM). Sinomenine was used because it is capable of increasing the bioavailability of paeoniflorin. In the rat perfusion model, absorption of paeoniflorin (50 μM) was increased in the jejunum (45–55%) and terminal ileum (80–86%) but not in duodenum (Fig. 5A) by these inhibitors. On the other hand, only cyclosporine A was able to significantly increase the absorption of paeoniflorin in the colon (38%) (Fig. 5A).

Unlike their effect on the absorption, cyclosporine A and sinomenine had minimal impact on the percentages of metabolites (paeoniflorigenin and benzoic acid) found in the small intestine (Fig. 5B). In the colon, percentages of paeoniflorigenin found significantly decreased although the extent of decrease is quite small (<25%) (Fig. 5B). On the other hand, colonic excretion of benzoic acid did not change in the presence of cyclosporine A or sinomenine (Fig. 5C).

Caco-2 Cell Culture Model Studies

The Caco-2 cell culture model is well recognized and commonly used model of the human intestine. The special feature of this model is that both apical and basolateral sides of the intestinal epithelium are easily accessible and therefore is excellent model for studying drug excretion or efflux.

Vectorial Transport of Paeoniflorin in Caco-2 Cell Monolayers

Amount of transported paeoniflorin increased linearly with time and was vectorial (or loading side dependent)

Table II. Effects of Sinomenine and ABC Transporter Inhibitors on the Transepithelial Transport of Paeoniflorin

Inhibitor	Concentration (μM)	Rate of transport (pmol min^{-1} cm^{-2}) A-B (mean ± SD) (% control ± SD)	Rate of transport (pmol min^{-1} cm^{-2}) B-A (mean ± SD) (% control ± SD)	Ratio (B-A/A-B)
None (control)	–	2.94 ± 0.11 (100.00 ± 3.74)	8.13 ± 0.48 (100.00 ± 5.90)	2.76
+Cyclosporin A	5	4.14 ± 0.43** (140.82 ± 14.63)	5.14 ± 0.30** (63.22 ± 3.69)	1.24
+Verapamil	100	3.73 ± 0.58* (126.87 ± 19.73)	5.29 ± 0.52** (65.07 ± 6.40)	1.42
+Leukotriene C(4) and MK-571	0.1+50	3.12 ± 0.37 (106.12 ± 12.58)	8.07 ± 0.53 (99.26 ± 6.51)	2.79
+Sinomenine	100	4.05 ± 0.40** (137.76 ± 13.61)	4.03 ± 0.52** (49.57 ± 6.40)	0.99

The AP-to-BL and BL-to-AP transport of paeoniflorin (100 μM) across Caco-2 cell monolayers in the absence (control) or presence of 100-μM sinomenine, 5-μM cyclosporin A or 100-μM verapamil was examined. The rates of transepithelial transport for both AP-to-BL and BL-to-AP transport were calculated as described in the Materials and Methods section. Data are expressed as mean ± SD, and $n = 3$. The statistically significant difference is between rates in the absence (none) or presence of an inhibitor.
**$P < 0.01$.
*$P < 0.05$.

(Table I). In the absence of ABC transporter inhibitors or sinomenine, basolateral to apical (BL-to-AP) or secretory transport of paeoniflorin was higher than ($p < 0.01$) that of apical to basolateral (AP-to-BL) or absorptive transport (Table I). At a concentration of 100 μM, the B-A/A-B transport ratio was approximately 3 with an AP-to-BL transport rate of 2.94 ± 0.11 pmol min^{-1} cm^{-2} and BL-to-AP rate of 8.13 ± 0.48 pmol min^{-1} cm^{-2} (Table I).

Effects of Concentration on the Vectorial Transport of Paeoniflorin

The rate of transepithelial transport of paeoniflorin increased with concentration (Table I). Although both AP-to-BL and BL-to-AP transport rates increased with concentration, the rates of BL-to-AP transport were always higher (Table I). The transport ratio (B-A/A-B) was fairly stable at 3, as the concentration of paeoniflorin increased from 100 to 800 μM (Table I).

Effects of Concentration on the Cellular Accumulation of Paeoniflorin

Cellular accumulation of paeoniflorin was assessed as a function of concentration (100–800 μM) (Fig. 6). The results showed that the levels of the accumulation increased with concentration until 400 μM, after which a further increase in the concentration did not result in further increase in the level of the accumulation. As expected, the levels of the accumulation following the BL loading were higher than those following the AP loading ($p < 0.05$).

Effects of Sinomenine and ABC Transporter Inhibitors on the Transport of Paeoniflorin

We used sinomenine, two MRP inhibitors and two P-gp inhibitors to determine how each inhibitor affected the transepithelial transport of paeoniflorin. The results indicated that prototypical p-gp inhibitors (e.g., verapamil, and cyclosporine A) significantly ($p < 0.05$) increased AP-to-BL transport and decreased BL-to-AP transport (Table II). In particular, BL-to-AP transport of paeoniflorin was inhibited 37% ($p < 0.01$) by 5-μM cyclosporine A, 35% by 100-μM verapamil ($p < 0.01$), 50% by 100-μM sinomenine ($p < 0.01$). Whereas AP-to-BL transport of paeoniflorin was enhanced 41% by 5-μM cyclosporine A ($p < 0.01$), 27% by 100-μM verapamil ($p < 0.01$), 38% by sinomenine ($p < 0.01$). The vectorial transport ratio in the presence of an effective inhibitor was approximately 1 (1.24 for cyclosporine A, 1.42 for verapamil, and 0.99 for sinomenine, respectively), where-

Table III. Intracellular Accumulation of Paeoniflorin in the Presence of Sinomenine and P-gp Inhibitors

Inhibitor	Concentration (μM)	Cellular accumulation (pmol/monolayer) Apical loading (mean ± SD) (% control ± SD)	Cellular accumulation (pmol/monolayer) Basolateral loading (mean ± SD) (% control ± SD)	Ratio (B-A/A-B)
None (control)	–	129.5 ± 17.5 (100.00 ± 13.51)	170.0 ± 16.0 (100.00 ± 5.95)	1.32
Cyclosporin A	5	408.4 ± 33.1** (315.37 ± 25.60)	152.9 ± 7.5 (88.94 ± 4.41)	0.37
Verapamil	100	315.89 ± 6.42** (243.93 ± 83.32)	150.83 ± 12.9 (88.72 ± 4.35)	0.48
Sinomenine	100	229.9 ± 16.91** (177.54 ± 13.05)	177.78 ± 17.78 (104.58 ± 10.5)	0.78

The cellular accumulation of paeoniflorin (100 μM) in Caco-2 cell monolayers in the absence of any inhibitor (control), or in the presence of 100-μM sinomenine, 5-μM cyclosporin A or 100-μM verapamil was determined with apical and basolateral loading. The apical buffer was at pH 6.5 HBSS, and basolateral buffer was at pH 7.4 HBSS. After transport studies (4 h), Caco-2 monolayer cells were gently washed for three times with ice-cold HBSS (pH 7.4) buffer and then cut off along with the polycarbonate filters. The cells were then broken up via sonication and the lysates were used for measuring the amounts of paeoniflorin inside cells. The obtained values were normalized by the control value to get relative paeoniflorin accumulation levels in Caco-2 monolayer cells. Data are expressed as mean ± SD, and $n = 3$. The statistically significant difference is between rates in the absence (none) or presence of an inhibitor.
**$P < 0.01$.

Table IV. The Concentration-Dependent Effects of Sinomenine on the Transport of Paeoniflorin Across Caco-2 Cell Monolayers

Sinomenine (μM)	Rate of transport (pmol min^{-1} cm^{-2})		Ratio (B-A/A-B)
	A-B (mean ± SD)	B-A (mean ± SD)	
–	2.94 ± 0.11 (100.00 ± 3.74)	8.13 ± 0.48 (100.00 ± 5.90)	2.76
50	3.32 ± 0.15 (112.93 ± 5.10)	7.19 ± 0.93 (88.44 ± 11.44)	2.17
100	4.05 ± 0.40** (137.76 ± 13.61)	4.03 ± 0.52** (49.57 ± 6.40)	0.99
150	4.25 ± 0.71** (144.56 ± 24.15)	5.78 ± 0.55** (71.09 ± 6.77)	1.36

The statistically significant difference is between the control (no sinomenine) and the sinomenine-treated cells. The AP-to-BL and BL-to-AP transport of paeoniflorin (100 μM) across Caco-2 cell monolayers as a function of sinomenine concentrations were measured, and the rates of transepithelial transport for both AP-to-BL and BL-to-AP transport were calculated as described in the Materials and Methods section. Data are expressed as mean ± SD for transport values, and $n = 3$.
**$P < 0.01$.

as the ratio in the absence of inhibitors was approximately 2.76. A transport ratio of 0.99, resulted from the inhibition of sinomenine, indicates there was a complete inhibition of efflux by 100-μM sinomenine (Table II). In contrast, MRP inhibitors MK-571 + leukotriene C4 did not affect the transport of paeoniflorin.

Effects of Sinomenine or P-gp Inhibitors on the Accumulation of Paeoniflorin

We also determined intracellular accumulation of paeoniflorin in the presence of p-gp inhibitors or sinomenine (Table III). Effective inhibitors of p-gp always increased the intracellular drug concentration to a higher level when paeoniflorin was loaded apically. The highest level of accumulation was achieved in the presence of 5 μM cyclosporine A. On the other hand, when loaded basolaterally the accumulation of paeoniflorin was only marginally affected by the presence of effective p-gp inhibitors, and the maximal decrease was only 11% ($p > 0.05$).

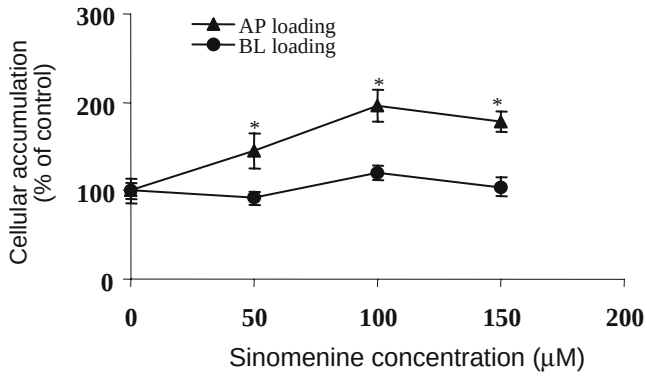

Fig. 7. The concentration-dependent effects of sinomenine on paeoniflorin accumulation (% control) in Caco-2 monolayer cells. The AP loaded (*filled triangle*) and BL loaded (*filled circle*) cellular accumulation of paeoniflorin (100 μM) in Caco-2 cell monolayers in the presence of increasing concentrations of sinomenine. After transport studies (2 h), Caco-2 monolayer cells were gently washed for three times with iced HBSS (pH 7.4) buffer and then cut off along with the polycarbonate filters. The cells were then sonicated at 4°C for 15 min and centrifuged at 13,000 rpm for 10 min to produce cell lysate for measuring the amount of digoxin in cellular accumulation. The control values were actually higher for BL loading than AP loading as shown in Table III. The *asterisk* (*) indicates a statistically significant difference in cellular accumulation between control and higher concentration of sinomenine. Each data point is the average of three determinations, and the *error bars* represent the standard deviation of the mean.

Concentration-dependent Effects of Sinomenine on the Transport of Paeoniflorin

We determined the transepithelial transport of paeoniflorin in the presence of increasing concentrations of sinomenine. As shown in Table IV, the effects of sinomenine were shown to be concentration-dependent and significant ($p < 0.05$) effects were observed at 50 μM of sinomenine for both AP-to-BL and BL-to-AP transport (Table IV). A concentration of 100-μM sinomenine had the strongest effect on paeoniflorin transport with a complete inhibition of transporter-mediated efflux.

Concentration-dependent Effects of Sinomenine on the Accumulation of Paeoniflorin

Cellular accumulation (4 h) of paeoniflorin in Caco-2 monolayer cells was also measured in the presence of sinomenine with increasing concentrations (Fig. 7). The increasing accumulation was shown to be sinomenine concentration-dependent (Fig. 7) with significant effects produced even at the lowest concentration tested (50 μM).

Paeoniflorgenin (Aglycone) versus Paeoniflorin (Glucoside)

As expected, there were huge differences in the transport properties between paeoniflorin (glucoside) and paeoniflorigenin (aglycone). As shown in Fig. 8 and Table V, the AP-to-BL transport rate at 100 μM was 44 times higher ($p < 0.001$) (129.09 ± 5.95 pmol min^{-1} cm^{-2} for aglycone, 2.94 ± 0.11 pmol min^{-1} cm^{-2} for glucoside). The BL-to-AP transport rate was 17 times higher for 100-μM paeoniflorigenin (138.56 ± 9.98 pmol min^{-1} cm^{-2} for aglycone, 8.13 ± 0.48 pmol min^{-1} cm^{-2}) ($p < 0.001$) than that of paeoniflorin (8.13 ± 0.48 pmol min^{-1} cm^{-2} for glucoside). As expected, cellular accumulations of paeoniflorigenin, regardless of its loading side, were also higher ($p < 0.001$) than that of paeoniflorin (Table V). Regardless of transport or accumulation, paeoniflorigenin showed little vectorial effects.

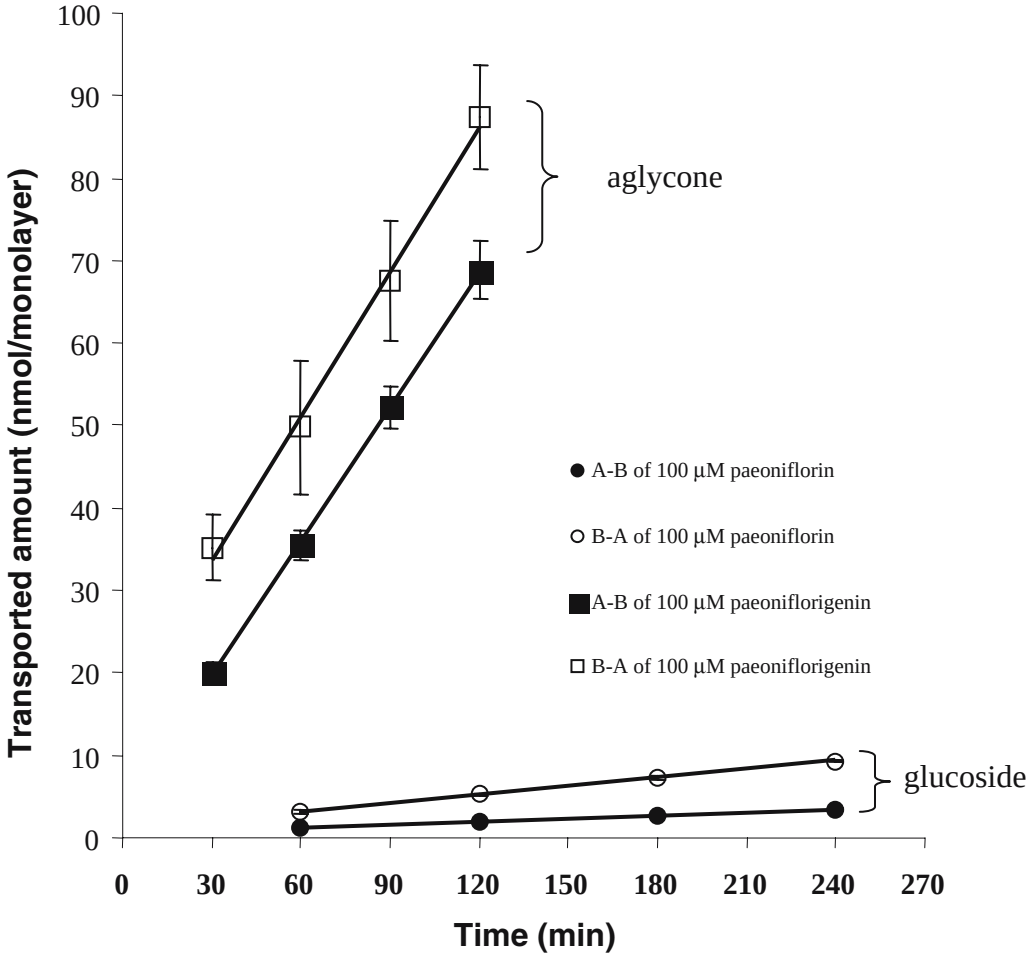

Fig. 8. Transport of paeoniflorin (glucoside, *circle symbols*) and paeoniflorigenin (aglycone, *square symbols*) in the Caco-2 cell model ($n = 3$). Transport across the Caco-2 cell culture model was performed at 37°C for 4 h for the glucoside and 2 h for the aglycone. Transports in the absorptive direction (AP-to-BL) are represented by *solid symbols* whereas those in the opposite direction (BL-to-AP) are represented by the *hollow symbols*. Each data point represents the average of three determinations and the *error bar* represents the standard deviation of the mean.

Table V. Permeabilities of Paeoniflorin and Paeoniflorigenin and Amounts of Their Transport in the Caco-2 Model ($n = 3$)

	Permeability (10^{-6} cm/s)		Rate of transport (pmol min^{-1} cm^{-2})			Amount of accumulation (pmol/monolayer)		
Compound	A-B (mean ± SD)	B-A (mean ± SD)	A-B (mean ± SD)	B-A (mean ± SD)	Ratio (B-A/A-B)	A-B (mean ± SD)	B-A (mean ± SD)	Ratio (B-A/A-B)
Paeoniflorin (100 μM)	0.483 ± 0.018	1.396 ± 0.008	2.94 ± 0.11	8.13 ± 0.48	2.77	129.47 ± 35.07	169.77 ± 31.60	1.31
Paeoniflorigenin (100 μM)	23.00 ± 1.51*	23.54 ± 1.70*	129.09 ± 8.44*	138.56 ± 9.98*	1.07	1,128.78 ± 74.92*	1,402.95 ± 59.20*	1.24

Amount of paeoniflorin transported at the end of 4-h experiments, and amount of paeoniflorgenin transport at the end of 2-h experiments were determined. After transport studies (4 h for paeoniflorin and 2 h for paeoniflorgenin), Caco-2 monolayer cells were gently washed for three times with iced HBSS (pH 7.4) buffer and then cut off insert along with the polycarbonate filters. The cells were then sonicated at 4°C for 15 min and centrifuged at 13,000 rpm for 10 min to produce cell lysate for measuring the amounts of paeoniflorin accumulation inside cells. Permeability values were calculated using the data in the amount transported *versus* time plot (Fig. 8). Data are expressed as mean ± SD, and $n = 3$. The statistically significant difference is between paeoniflorin and paeoniflorgenin.
*$P < 0.001$.

Table VI. Concentration-Dependent Effects of Sinomenine on the Transport of Digoxin Across Caco-2 Cell Monolayers

Sinomenine (μM)	Rate of transport (pmol min^{-1} cm^{-2}) A-B (mean ± SD)	B-A (mean ± SD)	Ratio (B-A/A-B)
–	1.59 ± 0.17	4.32 ± 0.39	2.72
50	1.73 ± 0.17	3.11 ± 0.15*	1.79
100	2.14 ± 0.19*	2.67 ± 0.20**	1.24

The AP-to BL and BL-to-AP transport of digoxin (40 μM) across Caco-2 cell monolayers in the presence of increasing concentrations of sinomenine was measured, and the rates of transepithelial transport values for both AP-to-BL and BL-to-AP transport were calculated as described in the Materials and Methods section. Data are expressed as mean ± SD for transport values, and $n = 3$. The statistically significant difference is between the control (no sinomenine) and the sinomenine-treated cells.
*$P < 0.05$.
**$P < 0.01$.

Concentration-dependent Effects of Sinomenine on the Transport of Digoxin

The effects of sinomenine on transport of digoxin, a prototypical p-gp substrate, were investigated to determine how sinomenine may interact with paeoniflorin. As shown in Table VI, the effects of sinomenine were shown to be concentration-dependent, and significant ($p < 0.05$) effects could be observed at the lowest tested concentration (50 μM) (Table VI). Sinomenine at 100 μM had the strongest inhibitory effect on digoxin transport, but it was unable to completely block P-gp at the tested concentrations.

Transport of Sinomenine in Caco-2 Cell Monolayers

To determine if sinomenine is a substrate of efflux transporter, we measured its AP-to-BL and BL-to-AP transport at several concentrations. The results indicated that BL-to- AP of sinomenine was always similar to that of AP-to-BL or displayed no vectorial transport (Table VII). At the lowest tested concentration of 10 μM, the ratio of B-A/A-B was approximately 1, which did not change when sinomenine concentration gradually increased to 80 μM (Table VII).

DISCUSSION

This is a comprehensive study that employed both animal and human intestinal models to further characterize the absorption and metabolism characteristics of paeoniflorin. These models allowed us to systematically delineate the mechanistic processes that influence the intestinal transport and metabolism of paeoniflorin. Our results indicated that poor permeation, p-glycoprotein-mediated efflux, and hydrolysis to the aglycones and benzoic acids all contribute to the poor bioavailability of paeoniflorin.

In the first set of studies, absorption of paeoniflorin was shown to be very poor and its permeability was much lower than those of highly permeable compounds such as propranolol and testosterone. In the Caco-2 cell culture model, permeability of paeoniflorin ($P_{app\ A\text{-}B} = 0.48 \times 10^{-6}$ cm/s) was 23 times lower than that of propranolol (11.3×10^{-6} cm/s) (20), and more than 60 times lower than that of testosterone (33×10^{-6} cm/s) (20). On the other hand, paeoniflorin permeability was similar to those of poorly absorbed compounds such as mannitol (1.7×10^{-6} cm/s) (20) and sulfasalazine (0.34×10^{-6} cm/s) (24). Similarly, in the perfused rat intestinal model, permeability of paeoniflorin ($P^*_{eff} < 0.4$ in all four intestine segments, Fig. 3) was also much lower than propranolol ($P^*_{eff} > 3.5$). Paeoniflorin's permeability was, however, similar to that of poorly absorbed compounds such as rutin ($P^*_{eff} < 0.58$) and mannitol ($P^*_{eff} < 0.3$) (25). Taken together, these results suggest that low permeability of paeoniflorin is one of the reasons that this compound has poor bioavailability.

What is the cause of this low permeation? The first reason is probably due to its low lipophilicity since the compound has a low partition coefficient (log PC = −2.88). We also determined if its permeation was further limited by drug efflux pumps expressed on the apical membrane of enterocytes (11). The results of this study clearly demonstrated the presence of an efflux transporter-mediated secretory transport of paeoniflorin in Caco-2 cell monolayers (Table I). To determine the efflux transporter responsible, several p-gp inhibitors (e.g., cyclosporine A and verapamil) and MRP inhibitors were used, but only cyclosporine A and verapamil were shown to be effective in decreasing the BL-

Table VII. Effects of Concentration on the Transepithelial Transport of Sinomenine

Sinomenine (μM)	Rate of transport (pmol min^{-1} cm^{-2}) A-B (mean ± SD)	B-A (mean ± SD)	Ratio (B-A/A-B)
10	16.76 ± 0.76	18.43 ± 1.57	1.15
20	22.22 ± 0.66	21.06 ± 1.55	0.93
40	37.43 ± 4.07	37.62 ± 1.15	0.87
60	43.85 ± 3.09	42.17 ± 3.01	0.98
80	62.90 ± 3.48	64.14 ± 4.91	0.94

Experiments were performed at 37°C for 2 h using protocol described earlier in Table VI. Rates of transepithelial transport in AP-to-BL and BL-to-AP direction were calculated as described in the Materials and Methods section. Data are expressed as mean ± SD, and $n = 3$.

to-AP transport of paeoniflorin and increasing the AP-to-BL transport (Tables II and III). These inhibitors diminished or abolished the loading side-dependent transport and cellular accumulation (Tables II and III). Although cyclosporine A is a potent p-gp inhibitor, it may have affected BCRP. On the other hand, verapamil did not affect the transport of BCRP substrate in a cell line that overexpressed it (26). Taken together, p-gp is likely an efflux transporter responsible for pumping out paeoniflorin at the apical membrane of the Caco-2 cells.

The involvement of p-gp, as demonstrated in the Caco-2 model, is also shown using the perfused rat intestinal model. For example, absorption of paeoniflorin in rat intestine was also enhanced by cyclosporine A and this enhancing effect was the most pronounced in the terminal ileum (Fig. 5A). P-gp is highly expressed on the apical surface of the ileal and colonic epithelial cells, and expression gradually decreases toward the stomach (27–29). On the other hand, BCRP is more evenly expressed across the different regions of the intestine (27–29). In contrast, MPR2 is also expressed at the apical surface but its expression level is highest in the duodenum and expression decreases toward ileum (30). Taken together, these results are consistent with our observation is Caco-2 cell culture model, where efflux via p-gp is likely the major mechanism that impedes the permeation of paeoniflorin in the rat small intestine, although we cannot fully discount the possibility that BCRP is also involved.

In addition to poor permeation, metabolism of paeoniflorin is another important mechanism that is responsible for poor bioavailability of paeoniflorin. A predominant intestinal metabolite of paeoniflorin is paeoniflorigenin (the aglycone of paeoniflorin), which represented a significant portion of the paeoniflorin (up to 42%) that apparently absorbed or disappeared from the perfusate (Fig. 3). The large extent of hydrolysis in the intestine suggests that the brush-border glucosidase LPH represents a significant barrier to the absorption of intact paeoniflorin. By using LPH inhibitor gluconolactone, we were able to show that hydrolysis to the aglycone decreased substantially (>80%), which translated also into much lower apparent absorption in the upper small intestine where LPH is more active (Fig. 4). Since aglycone is 48 times more permeable than glucoside (Table V), the results of gluconolactone experiment suggest that a substantial amount of glucoside disappearance from the upper small intestine is through its hydrolysis first into the aglycone and then absorbed as aglycone. This mechanism is similar to what we observed in the intestinal absorption of flavonoid glucosides such as apigetrin, genistin, and isoquercetrin (25). Because paeoniflorin is extensively metabolized into paeoniflorigenin, it would be valuable to study the pharmacological effects of paeoniflorigenin to determine if the highly absorbed aglycone is itself active. If it is active, we could accordingly change the formulation or the processing method to maximize the presence of paeoniflorigenin in the medications.

Another important metabolic pathway is the esterase-catalyzed hydrolysis of paeoniflorin, which produces benzoic acid (Figs. 3 and 4). In terms of extent, the esterase-catalyzed hydrolysis is approximately one-third of the LPH-catalyzed hydrolysis. Therefore, esterases are less important than LPH, especially in light of the fact that some of the benzoic acid excreted may come from paeoniflorin not paeoniflorigenin.

In our study, sinomenine was always effective in enhancing the transport of paeoniflorin (Fig. 5, Table IV), which is consistent with an earlier observation that sinomenine significantly increased (more than 12 times) the paeoniflorin bioavailability in rats (5). What is the mechanism for this enhanced transport and/or bioavailability? Is it due to decrease in efflux or decrease in metabolism or both? The results indicated that sinomenine significantly increased the AP-to-BL transport of paeoniflorin and diminished vectorial transport (Table II). The results also indicated that sinomenine enhanced the transport and accumulation of digoxin (a prototypical p-gp substrate) in Caco-2 cell model (Table VI). Taken together, these results suggest that the alkaloid sinomenine may be a potentially novel inhibitor of p-gp, even though it is not a p-gp substrate itself. It may be used to increase the absorption/bioavailability of co-administrated p-gp substrates. Therefore, these results suggest that the use of this novel p-gp inhibitor could facilitate the development of an oral paeoniflorin product by combining paeoniflorin and sinomenine, the latter is also active for treating arthritis. To use sinomenine as a general p-gp inhibitor in humans, however, we need to demonstrate the safety of sinomenine as a modulator of p-gp in additional research.

In summary, the causes of paeoniflorin's poor bioavailability include poor permeation due to lack of lipophilicity, efflux via p-gp, and hydrolytic degradation in the intestinal brush border by LPH and certain esterases. Bioavailability of paeoniflorin may be improved by inhibiting the efflux transporter (e.g., sinomenine) and perhaps by using LPH inhibitors (e.g., gluconolactone). Our present study suggests that it is necessary to determine if the more bioavailable form of paeoniflorin, its aglycone paeoniflorigenin, has superior pharmacological activities.

ACKNOWLEDGMENTS

This work was supported by grants (ZQL, LL, ZHJ) of JCICM-6-02 from the Hong Kong Jockey Club Charities Trust of Hong Kong and of CA-87779 (MH) from the National Institutes of Health, USA. This work was conducted at University of Houston, College of Pharmacy during a research visit by ZQL. The authors wish to thank Drs. Hong Xi Xu and Hua Zhou for their supports and comments to this work.

REFERENCES

1. J. Yamahara, T. Yamada, H. Kimura, T. Sawada, and H. Fujimura. Biologically active principles of crude drug. II. Anti-allergic principles in "Shoseir-yu-To" anti-inflammatory properties of paeoniflorin and its derivatives. *J. Pharmacobio-Dyn.* **5**:921–929 (1982).
2. M. Kimura, I. Kimura, and H. Nojima. Depolarizing neuromuscular blocking action induced by electropharmacological coupling in the combined effect of paeoniflorin and glycyrrhizin. *Jpn. J. Pharmcol.* **37**:395–397 (1984).
3. S. Takeda, T. Isono, Y. Wakui, Y. Matsuzaki, H. Sasaki, and S. Amagaya. Absorption and excretion of paeoniflorin in rats. *J. Pharm. Pharmacol.* **47**:1036–1040 (1995).
4. S. Takeda, T. Isono, Y. Wakui, Y. Mizuhara, S. Amagaya, M. Maruno, and M. Hattori. *In-vivo* assessment of extrahepatic metabolism of paeoniflorin in rats: relevance to intestinal floral metabolism. *J. Pharm. Pharmacol.* **49**:35–39 (1997).

5. Z. Q. Liu, H. Zhou, L. Liu, Z. H. Jiang, Y. F. Wong, Y. Xie, X. Cai, H. X. Xu, and K. C. Chan. The pharmacokinetic fate of paeoniflorin influenced by co-administration of sinomenine in unrestrained conscious rats. *J. Ethnopharmaco.* **99**:61–67 (2005).
6. L. C. Chen, M. H. Lee, M. H. Chou, M. F. Lin, and L. L. Yang. Pharmacokinetic study of paeoniflorin in mice after oral administration of *Paeoniae radix* extract. *J. Chromatogr. B.* **735**:33–40 (1999).
7. L. C. Chen, M. H. Chou, M. F. Lin, and L. L. Yang. Pharmacokinetics of paeoniflorin after oral administration of Shao-yao Gan-cha Tang in mice. *Jpn. J. Pharmacol.* **88**:250–255 (2002).
8. S. L. Hsiu, Y. T. Lin, K. C. Wen, Y. C. Hou, and P. D. Chao. A deglucosylated metabolite of paeoniflorin of the root of *Paeonia lactiflora* and its pharmacokinetics in rats. *Planta Med.* **69**:1113–1118 (2003).
9. M. Hattori, Y. Z. Shu, M. Shimizu, T. Hayashi, N. Morita, X. G. Kobashi, and T. Namba. Metabolism of paeoniflorin and related compounds by human intestinal bacteria. *Chem. Pharm. Bull.* **33**:3838–3846 (1985).
10. Y. Z. Shu, M. Hattori, T. Akao, K. Kobashi, K. Kagi, K. Fukuyama, T. Tsukihara, and T. Namba. Metabolism of paeoniflorin and related compounds by human intestinal bacteria. II. Structures of 7S-and 7R-paeonimetabolines I and II formed by *Bacteroides fragillis* and *Lactobacillus brevis*. *Chem. Pharm. Bull.* **35**:2733–3726 (1987).
11. K. Chan, Z. Q. Liu, Z. H. Jiang, H. Zhou, Y. F. Wong, H. X. Xu, and L. Liu. The effects of sinomenine on intestinal absorption of paeoniflorin by everted rat gut sac model. *J. Ethnopharmacol.* **103**:425–432 (2006).
12. Z. Tai and S. J. Hopkins. Sinomenine: antiarthritic antiinflammatory. *Drugs of the Future* **23**:45–49 (1998).
13. L. Liu, J. Riese, K. Resch, and V. Kaever. Impairment of macrophage eicosanoid and nitric oxide production by sinomenine, an alkaloid from *Sinomenium acutum*. *Arzneim.-Forsch.* **44** (11): 1223–1226 (1994).
14. B. Vieregge, K. Resch, and V. Kaever. Synergistic effects of the alkaloid sinomenine in combination with the immunosuppressive drugs tacrolimus and mycophenolic acid. *Planta Med.* **44**:1223–1226 (1999).
15. L. Liu, K. Resch, and V. Kaever. Inhibition of lymphocyte proliferation by the anti-rheumatic drug sinomenine. *Int. J. Immunopharmacol.* **16**:685–691 (1996).
16. M. Hu, J. Chen, D. Tran, Y. Zhu, and G. Lenonardo. The Caco-2 cell monolayers as an intestinal metabolism model: metabolism of dipeptide Phe-Pro. *J. Drug Target.* **2**:79–89 (1994).
17. M. Hu, J. Chen, Y. Zhu, A. H. Dantzig, R. E. Stratford, and M. T. Kuhfeld. Mechanism and kinetics of transcellular transport of a new β-lactam antibiotic loracarbef across an human intestinal epithelial model system (Caco-2). *Pharm. Res.(NY)* **11**:1405–1413 (1994).
18. J. Chen, H. Lin, and M. Hu. Metabolism of flavonoids via enteric recycling: role of intestinal disposition. *J. Pharmacol. Exp. Ther.* **304**:1228–1235 (2003).
19. E. J. Jeong, X. B. Jia, and M. Hu. Disposition of formononetin via enteric recycling: metabolism and excretion in mouse intestinal perfusion and Caco-2 cell model. *Mol. Pharmacol.* **2**:319–328 (2005).
20. E. J. Jeong, Y. Liu, H. Lin, and M. Hu. *In situ* single-pass perfused rat intestinal model for absorption and metabolism. In Z. Yan and G. W. Caldwell (eds.), *In Methods in Pharmacology and Toxicology: Optimization in Drug Discovery—In Vitro Methods*, Human, Totowa, NJ, 2004, pp. 65–76.
21. M. Hu, K. Ge, L. Roland, J. Chen, P. Tyle, and S. Roy. Determination of absorption characteristics of AG337, a novel thymidylate synthase inhibitor, using a perfused rat intestinal model. *J. Pharm. Sci.* **87**:886–890 (1998).
22. M. Hu, P. J. Sinko, A. L. J. DeMeere, D. A. Johnson, and G. L. Amidon. Membrane permeability parameters for some amino acids and β-lactam antibiotics: application of the boundary layer approach. *J. Theor. Biol.* **131**:107–114 (1988).
23. T. Tanaka, S. Takase, and T. Goda. A possible role of a nuclear factor NF-LPH1 in the regional expression of lactase-phlorizin hydrolase along the small intestine. *J. Nutr. Sci. Vitaminol. (Tokyo)* **43**:565–573 (1997).
24. E. Liang, J. Proudfoot, and M. Yazdanian. Mechanisms of transport and structure–permeability relationship of sulfasalazine and its analogs in Caco-2 cell monolayers. *Pharm. Res.* **17**:1168–1174 (2000).
25. Y. Liu, Y. Liu, Y. Dai, L. Y. Xun, and M. Hu. Enteric disposition and recycling of flavonoids and ginkgo flavonoids. *J. Alter. Complement. Med.* **9**:631–640 (2003).
26. Y. Zhang, A. Gupta, H. Wang, L. Zhou, R. R. Vethanayagam, J. D. Unadkat, and Q. Mao. BCRP transports dipyridamole and is inhibited by calcium channel blockers. *Pharm. Res.* **22**: 2023–2034 (2005).
27. G. T. Ho, F. M. Moodie, and J. Satsangi. Multidrug resistance 1 gene (P-glycoprotein 170): an important determinant in gastrointestinal disease?. *Gut* **52**:759–766 (2003).
28. R. Tian, N. Koyabu, H. Takanaga, H. Matsuo, H. Ohtani, and Y. Sawada. Effects of grapefruit juice and orange juice on the intestinal efflux of P-glycoprotein substrates. *Pharm. Res.* **19**: 802–809 (2002).
29. Y. Tanaka, A. L. Slitt, T. M. Leazer, J. M. Maher, and C. D. Klaassen. Tissue distribution and hormonal regulation of the breast cancer resistance protein (Bcrp/Abcg2) in rats and mice. *Biochem. Biophys. Res. Commun.* **326**:181–187 (2005).
30. B. M. Johnson, P. Zhang, J. D. Schuetz, and K. L. Brouwer. Characterization of transport protein expression in multidrug resistance-associated protein (mrp) 2-deficient rats. *Drug Metab. Dispos.* **34**:556–562 (2006).